Influence of nucleation and dendrite fragmentation on as-cast structure of Sn-10wt.%Pb benchmark

Yongjian ZHENG[1], Menghuai WU[1, 2], Abdellah Kharicha[1, 2], Andreas Ludwig[1]
[1]Chair of Modeling and Simulation of Metallurgical Processes, University of Leoben, Austria
[2]Christian Doppler Lab for Advanced Simulation of Solidification and Melting, University of Leoben, Austria
E-mail: menghuai.wu@unileoben.ac.at

Key words: solidification, heterogeneous nucleation, dendrite fragmentation, simulation.

Abstract: A laboratory benchmark casting experiment on the Sn-10 wt.%Pb alloy has shown an equiaxed zone in the up-left region of the casting [Hachani et al., Int. J. Heat Mass Transfer, 85 (2015), 438-454]. It is not clear if the equiaxed crystals originate from heterogeneous nucleation or dendrite fragmentation. The current work is to use a three-phase mixed columnar-equiaxed solidification model to study its solidification process by assuming different crystal origins, due to either the heterogeneous nucleation, dendrite fragmentation, or a combination of them. Simulations are performed, and compared with the as-cast structure. The modeling results show that when the nucleation is considered as the sole origin of equiaxed crystals, it is difficult to 'reproduce' the experimental result, i.e. the calculated equiaxed zone is much narrower than the one of the as-cast structure. When the fragmentation is considered as the origin of equiaxed crystals, the shape of equiaxed zone seems closer to experimental one. The case with combination of nucleation and fragmentation show the best agreement with the experiment. Based on this modeling study, fragmentation seems to play a dominant role in the origin of equiaxed crystals.

Introduction

The laboratory solidification experiments were widely used to investigate the formation of as-cast structure and related phenomena [1, 2]. Recently, an experiment setup with precise control of cooling rate and temperature gradient was designed [3], and a series of solidification experiments and post-mortem metallographic analyses of as-solidified benchmarks were performed at the SIMAP Laboratory in Grenoble, France [4]. It reported that there was an equiaxed zone in the up-left region of the benchmark under normal gravity condition. A hypothesis is that solute-rich liquid rises through the mushy zone and causes re-melting and fragmentation, which may explain the origin of equiaxed crystals. Based on the theoretical study on local remelting of the mushy zone [5, 6], the authors have proposed a simple formula to consider the fragmentation phenomenon in a mixed columnar-equiaxed solidification model [7, 8]. The fragmentation rate is dependent on the local melt concentration gradient and the interdendritic flow. A preliminary study has shown that the equiaxed zone in the benchmark casting is reproducible by the numerical model if the fragmentation mechanism is considered [9]. It is also well known that the heterogeneous nucleation is an important crystal origin of many engineering castings [10]. Therefore, new questions arise: can the aforementioned as-cast structure be reproduced if only the heterogeneous nucleation is considered, and how does the as-cast structure look like if both fragmentation and heterogeneous nucleation are considered? To address above questions, the current work tries to use the same three-phase mixed columnar-equiaxed solidification model to analyze the solidification process with the emphasis on the transport of equiaxed crystals. Simulations are made with assumption of different crystal origins, due to either the heterogeneous nucleation, fragmentation, or a combination of them. The calculated mixed columnar-equiaxed structure is compared with the as-cast structure, hence to get some indications about the most probable mechanism of the origin of the equiaxed crystals.

Model descriptions

The three-phase mixed columnar-equiaxed solidification model was described previously [8]. The three phases are the primary melt (ℓ), equiaxed (e) and columnar phases (c). Their volume fractions are quantified by f_ℓ [-], f_e [-], and f_c [-], and $f_\ell + f_e + f_c = 1$. Both the liquid and equiaxed phases are

moving phases, and the corresponding Navier-Stokes equations are solved. The columnar phase is assumed to be rigid and stationary. Nucleation of equiaxed crystals is assumed to occur following a classical Gaussian heterogeneous nucleation law. The inoculants (n_{em} [m^{-3}]) serve as nucleation sites, which are activated as equiaxed crystals (n_{eq}[m^{-3}]) by undercooling (ΔT [K]) as follows:

$$N_{nu} = \frac{n_{em}}{n_{max}} \cdot \frac{D(\Delta T)}{D(t)} \cdot \frac{dn_{eq}}{d(\Delta T)} \quad (1)$$

$$\frac{D(\Delta T)}{D(t)} = \frac{\partial T}{\partial t} + u_\ell \cdot (m \cdot \frac{\partial c_\ell}{\partial x} - \frac{\partial T_\ell}{\partial x}) + v_\ell \cdot (m \cdot \frac{\partial c_\ell}{\partial y} - \frac{\partial T_\ell}{\partial y}) \quad (2)$$

$$\frac{dn_{eq}}{d(\Delta T)} = \frac{n_{max}}{\sqrt{2\pi}\cdot\Delta T_\sigma} \cdot e^{-\frac{1}{2}(\frac{\Delta T - \Delta T_N}{\Delta T_\sigma})^2} . \quad (3)$$

N_{nu}, N_{max}, ΔT_N, ΔT_σ mean heterogeneous nucleation rate [m^{-3} s^{-1}], initial inoculant number density [m^{-3}], Gaussian distribution width [K] and undercooling for maximum grain production rate [K], respectively. u_ℓ, v_ℓ, c_ℓ, T_ℓ , m indicate x component of liquid velocity [m s^{-1}], y component of liquid velocity [m s^{-1}], liquid concentration [-], liquid temperature [K], and liquidus slope [-], respectively. The method to treat dendrite fragmentation in the mixed columnar-equiaxed solidification model was described elsewhere [7]. The fragmentation-induced mass transfer rate (M_{ce} [kg m^{-3} s^{-1}]) from columnar to the equiaxed is calculated:

$$M_{ce} = -\gamma \cdot (\vec{u}_\ell - \vec{u}_c) \cdot \nabla c_\ell \cdot \rho_e . \quad (4)$$

γ, ρ_e are the fragmentation coefficient [-] and equiaxed phase density [kg m^{-3}]. $\vec{u}_\ell$ and $\vec{u}_c$ denote liquid and columnar velocity vectors [m s^{-1}]. Note that fragmentation occurs only with remelting, i.e. for the case of $M_{ce} > 0.0$. For the case of solidification (calculated M_{ce} has a negative value), we set $M_{ce} = 0.0$, i.e. no fragmentation should occur. The mass integral of all fragments as produced per time is proportional to the increase rate of constitutional supersaturation as caused by the interdendritic flow. The diameter of the fragment ($d^0_{e,frag}$ [m]) is proportional to the secondary dendrite arm space (λ_2 [m]) and the volume fraction of the columnar phase (f_c):

$$d^0_{e,frag} = \lambda_2 \cdot f_c . \quad (5)$$

Hence the rate of the fragment production (N_{frag} [m^{-3} s^{-1}]) can be calculated as:

$$N_{frag} = \frac{M_{ce}}{\rho_e \cdot \frac{\pi}{6}(d^0_{e,frag})^3} . \quad (6)$$

The transport of equiaxed inoculants is calculated as follows [11, 12].

$$\frac{\partial}{\partial t} n_{em} + \nabla \cdot (\vec{u}_\ell n_{em}) = -N_{nu} . \quad (7)$$

As the columnar dendrite structure and the equiaxed grains (crystals) are treated as two separated solid phases, evolutions of them by solidification are calculated explicitly. The amounts of them are quantified by their volume fractions, f_c and f_e. The columnar phase is stationary ($\vec{u}_c = 0$). The motion of equiaxed crystals, $\vec{u}_e$, is calculated by solving corresponding momentum conservation equation. Transport of the number density of the equiaxed crystals, n_{eq}, must be calculated with

$$\frac{\partial}{\partial t} n_{eq} + \nabla \cdot (\vec{u}_e n_{eq}) = N , \quad (8)$$

by considering a source term N [m^{-3} s^{-1}]. N should include the contribution of the heterogeneous nucleation, N_{nu}, and the fragmentation, N_{frag}.

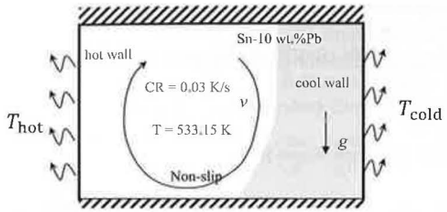

Figure 1. Simulation settings for the benchmark casting: geometry and boundary conditions.

Fig. 1 shows the configuration and settings of the simulation, as is in accordance with the experiment from Hachani et al. [4]. Sn-10 wt.%Pb alloy is considered. The thermodynamic and physical parameters can be found in reference [9]. 5 cases are calculated (Table 1). Case 1 assumes only the fragmentation as sole origin of equiaxed crystals, while Case 5 assumes heterogeneous nucleation as only origin. Case 2 to Case 4 consider both fragmentation and heterogeneous nucleation, with different nucleation parameters.

Table 1. Numerical parameter study and different simulation cases.

	origin of equiaxed crystals	parameters
Case 1	fragmentation only	$\gamma = 1.0$
Case 2	fragmentation + nucleation	N_{max}=5.0× 10^8 m^{-3}, ΔT_N =3.0 K, ΔT_σ = 3.0 K, γ = 1.0
Case 3	fragmentation + nucleation	N_{max}=1.0× 10^9 m^{-3}, ΔT_N =3.0 K, ΔT_σ = 3.0 K, γ = 1.0
Case 4	fragmentation + nucleation	N_{max}=5.0× 10^9 m^{-3}, ΔT_N =3.0 K, ΔT_σ = 3.0 K, γ = 1.0
Case 5	nucleation only	N_{max}=5.0× 10^9 m^{-3}, ΔT_N =3.0 K, ΔT_σ = 3.0 K

Results and discussion

Fig. 2 shows the simulated equiaxed zone in the as-solidified benchmark casting for different cases, as well as the as-cast structure of experiment observation. Contour in Fig. 2(a) shows the result of Case 1 (only fragmentation). There is an equiaxed zone in the up-left region, extending to the middle of the bottom. There is a small portion of equiaxed crystals which are scattered in the right part of the benchmark. The equiaxed crystals are set to be detached from the columnar trunk and some of them are embedded in the space between different columnar dendrites. If both fragmentation and nucleation are considered in the solidification process (Case 2-4), the position of equiaxed zone would not change significantly, locating in the up-left corner. However, the equiaxed area becomes broader as the initial inoculant number density n_{max} increases (Fig. 2(b)-(d)). When the initial inoculants number density is considered as $n_{max} = 5 \times 10^9$ m^{-3} (Case 4), the equiaxed zone is too large in comparison with the experiment (Fig. 2(d), (f)). The simulation result of Case 3 seems to show best agreement with the experiment using $n_{max} = 1 \times 10^9$ m^{-3} (Fig. 2(c), (f)). The fragmentation of dendrite plays a significant role in the formation of the equiaxed zone. The numerical analysis shows that without dendrite fragmentation, Case 5 even with a very large initial inoculant number density $n_{max} = 5 \times 10^9$ m^{-3} would not be able to reproduce the experiment result, i.e. the calculated equiaxed zone is too narrow (Fig. 2(e)).

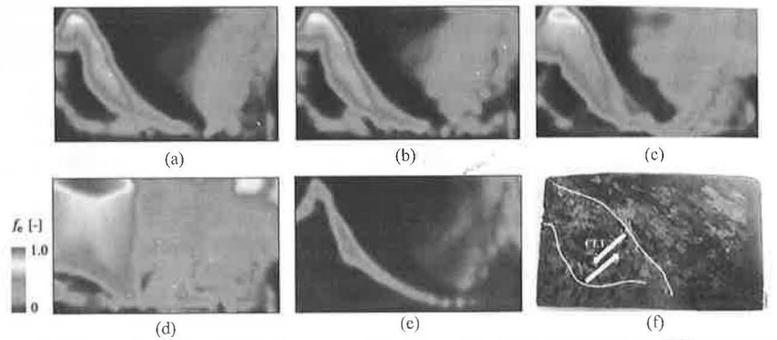

Figure 2. Calculated as-solidified equiaxed volume fraction contour for different cases with various parameters for equiaxed crystal origin and the as-cast structure of the experiment: (a) with fragmentation (Case 1), (b) with fragmentation and nucleation using $n_{max} = 5 \times 10^8$ m^{-3} (Case 2), (c) with fragmentation and nucleation using $n_{max} = 1 \times 10^9$ m^{-3} (Case 3), (d) with fragmentation and nucleation using $n_{max} = 5 \times 10^9$ m^{-3} (Case 4), (e) only with nucleation using $n_{max} = 5 \times 10^9$ m^{-3} (Case 5) and (f) as-solidified structure observed from experiment [4].

The subsequent analyses are based on Case 3. As shown in Fig. 2(f), an accumulated equiaxed zone was obtained in the up-left corner region of the as-solidified benchmark casting, and this region extends to the middle bottom. The transport of the equiaxed crystals is responsible for this distribution. Equiaxed crystals are produced near the solidification front. Subsequently, they tend to sediment along the columnar tip front due to the density difference between liquid and solid crystals. Meanwhile, the melt flow also tries to bring them into the bulk region (left side) and a large portion of equiaxed crystals would move into the melt bulk. As moving in the melt, those crystals continue to grow if the melt is still undercooled, or they might be melted if they are brought into the overheated or supersaturated region. As the density of the melt is strongly dependent on the solute enrichment of the melt [9], the equiaxed crystals are with different capability of settling due to the different density variation between solid and melt all over the benchmark.

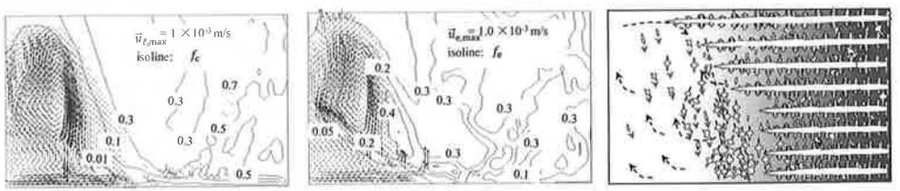

Figure 3. Analysis of the crystals movement for Case 3 during solidification at 2300 s: (a) liquid velocity field overlaid with f_e isoline; (b) equiaxed velocity overlaid with f_e isoline; (c) schematic of melt flow and equiaxed movement (black dash lines indicate the circulation of melt flow and red arrows indicate the relatively moving direction of equiaxed crystals).

A detailed analysis of the crystal movement for the moment at 2300 s is shown in Fig. 3. A clockwise liquid convection is observed in the melt. The intensity of the liquid flow is at the magnitude of 1×10^{-3} m s^{-1} (Fig. 3(a)). Due to the drag force between liquid and equiaxed crystals, the equiaxed crystals also form a clockwise convection (Fig. 3(b)), similar as that for the liquid. Equiaxed crystals tend to

move downwards relative to the liquid (Fig. 3(c)). The convection cell gradually shrinks and moves to the up-left corner, till the end of solidification. It is essential for the formation of final as-cast structure and the details are discussed in [9]. It is worth mentioning that no matter where the crystals come from, nucleation or fragmentation, the movement of crystals obeys a same pattern. It is impossible to figure out the origin of the crystal once it is formed.

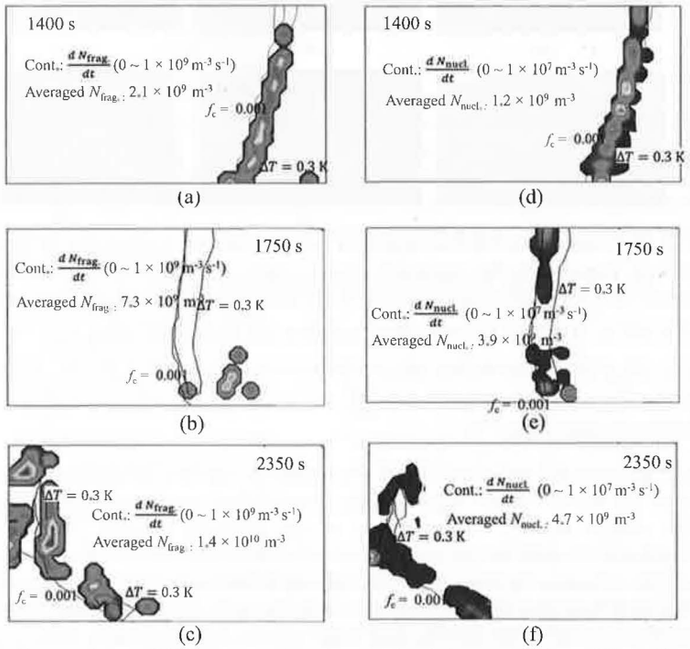

Figure 4. Comparison of different equiaxed crystal origin mechanisms (Case 3): (a)-(c) contours of fragmentation rate at 1400 s, 1750 s and 2350 s, respectively; (d)-(e) contours of heterogeneous nucleation rate at 1400 s, 1750 s and 2350 s, respectively.

Comparison of the differences equiaxed crystal origins, fragmentation or heterogeneous nucleation, are made in Fig. 4. At 1400 s, the solidification front advances to about ¼ length of the benchmark from right cold wall. Crystals form slightly behind the solidification front, either by the mechanisms of fragmentation or nucleation. The fragment production rate is about 100 times larger than heterogeneous nucleation rate (Fig. 4(a), (d)). When the solidification front evolves to the middle part of the benchmark (1750 s), the fragmentation is witnessed only in some special locations, e.g. bottom and segregated channels. This phenomenon is connected to the local liquid flow conditions. According to Eq. 4, the fragmentation is not available when the dot production of liquid concentration gradient ∇c_ℓ and liquid velocity $\vec{u}$ is equal or greater than zero. At this moment, the solidification front is nearly vertical (Fig. 4(b)), as would lead to a similar direction of liquid velocity. It would result in the unfavorable condition for fragmentation. However, the nucleation mechanism takes effect continuously (Fig. 4(e)) with a relatively low production rate with the magnitude 1×10^7 m^{-3} s^{-1}. At the late age of the solidification (2350 s), the fragmentation of dendrite plays an important role to produce equiaxed crystals in the mush zone. It happens in a wide area slightly behind the solidification front (Fig. 4(c)). Heterogeneous nucleation, by contrast, makes a contribution to the formation of equiaxed crystals near the front (Fig. 4(f)). The combined effect of fragmentation and nucleation would result in finally an enrichment equiaxed zone, as is close to the experiment observation. Even though the nucleation takes effect from the beginning to the end of solidification,

it is fragmentation that makes the dominant contribution to the crystals origination in the solidification process.

Summary discussion

Effects of heterogeneous nucleation and dendrite fragmentation on the formation of equiaxed zone in a solidifying Sn- 10% Pb benchmark were investigated by a three-phase mixed columnar-equiaxed solidification model. With undercooling the inoculants in the melt will be activated as equiaxed nuclei, and they can develop into equiaxed crystals. Remelting is the main mechanism for the origin of equiaxed fragments. Once the crystal is formed, it tends to settle down in the melt, interacting with the melt flow through the drag force. A clockwise convection cell shrinks and moves gradually to the up-left corner at the late age of solidification, as is responsible for the formation of equiaxed zone in the up-left part of the benchmark. It is difficult to reproduce the equiaxed zone properly only through the contribution of heterogonous nucleation. Even though the case only considering fragmentation can reproduce the shape and position of equiaxed zone, it is the case that properly considering both nucleation and fragmentation fits best with the experiment. Fragmentation plays the dominant role in the production of equiaxed crystals. Since the simulations were made in 2D, some details about the location of the crystal production were not properly revealed. For heterogonous nucleation, the Gaussian distribution width and undercooling for maximum grain production rate are given as fixed values. Additionally, a fixed value of 0.1 is assigned to fragmentation coefficient γ. Those parameters require further theoretic studies and experimental validations.

References

[1] D. Hebditch, J. Hunt, Observations of ingot macrosegregation on model systems, Metall. Mater. Trans., 5 (1974) 1557-1564.

[2] J. Sarazin, A. Hellawell, Channel formation in Pb-Sn, Pb-Sb, and Pb-Sn-Sb alloy ingots and comparison with the system NH4Cl-H2O, Metall. Mater. Trans. A, 19 (1988) 1861-1871.

[3] X. Wang, Y. Fautrelle, An investigation of the influence of natural convection on tin solidification using a quasi two-dimensional experimental benchmark, Int. J. Heat Mass Transfer, 52 (2009) 5624-5633.

[4] L. Hachani, K. Zaidat, Y. Fautrelle, Experimental study of the solidification of Sn–10 wt.%Pb alloy under different forced convection in benchmark experiment, Int. J. Heat Mass Transfer, 85 (2015) 438-454.

[5] M.C. Flemings, G.E. Nereo, Macrosegregation : Part I, Trans. Metall. Soc. Aime, 239 (1967) 1449-1462.

[6] T. Campanella, C. Charbon, M. Rappaz, Grain refinement induced by electromagnetic stirring: A dendrite fragmentation criterion, Metall. Mater. Trans. A, 35 (2004) 3201-3210.

[7] Y. Zheng, M. Wu, A. Kharicha, A. Ludwig, Incorporation of fragmentation into a volume average solidification model, Model. Simul. Mater. Sci. Eng., 26 (2018) 015004

[8] M. Wu, A. Ludwig, A three-phase model for mixed columnar-equiaxed solidification, Metall. Mater. Trans. A, 37A (2006) 1613-1631.

[9] Y. Zheng, M. Wu, E. Karimi-Sibaki, A. Kharicha, A. Ludwig, Use of a mixed columnar-equiaxed solidification model to analyse the formation of as-cast structure and macrosegregation in a Sn-10 wt% Pb benchmark experiment, Int. J. Heat Mass Transfer, 122 (2018) 939-953.

[10] M. Rappaz, Modelling of microstructure formation in solidification processes, Int. Mater. Rev., 34 (1989) 93-124.

[11] M. Wu, Y. Zheng, A. Kharicha, A. Ludwig, Numerical analysis of macrosegregation in vertically solidified Pb-Sn test castings–Part I: Columnar solidification, Comp. Mater. Sci., 124 (2016) 444-455.

[12] Y. Zheng, M. Wu, A. Kharicha, A. Ludwig, Numerical analysis of macrosegregation in vertically solidified Pb-Sn test castings–Part II: Equiaxed solidification, Comp. Mater. Sci., 124 (2016) 456-470.